The anisotropic structure of turbulence and its energy spectrum

G. E. Elsinga and I. Marusic

Citation: Physics of Fluids **28**, 011701 (2016); doi: 10.1063/1.4939471
View online: http://dx.doi.org/10.1063/1.4939471
View Table of Contents: http://scitation.aip.org/content/aip/journal/pof2/28/1?ver=pdfcov
Published by the AIP Publishing

The anisotropic structure of turbulence and its energy spectrum

G. E. Elsinga[1,a)] and I. Marusic[2]
[1]*Laboratory for Aero and Hydrodynamics, Delft University of Technology, 2628CA Delft, The Netherlands*
[2]*Department of Mechanical Engineering, The University of Melbourne, Victoria 3010, Australia*

The spectral energy distribution in turbulent flows is observed to follow a $k^{-5/3}$ power scaling, as originally predicted by Kolmogorov's theory. However, the underlying assumptions in Kolmogorov's theory appear not to hold with most experimental and numerical data showing evidence of small-scale anisotropy and significant direct energy transfer between the large- and the small-scales. Here, we present a flow structure that reconciles the $k^{-5/3}$ spectrum with small-scale universality, small-scale anisotropy, and direct scale interactions. The flow structure is a shear layer, which contains the small-scales of motion and is bounded by the large-scales. The anisotropic shear layer reveals the expected scaling of the energy spectrum in nearly all directions.

The phenomenology of turbulence involves fluid motion at a broad range of length scales. Together these motions produce the density variations in interstellar gasses,[1,2] disperse pollution in the atmosphere,[3,4] or increase wall friction, which can cause damage of artery tissue.[5,6] The accurate modeling of these physical processes depends on how the turbulent scales interact in physical space and their respective energies. Concerning the latter, the distribution of turbulent kinetic energy across the scales, represented by their wavenumber k, has been shown to follow a $k^{-5/3}$ power scaling. This $-5/3$rd power slope has been predicted from Kolmogorov's theory[7–9] and is strongly supported from measurements in various flows,[10–12] enforcing it as a defining property of turbulence. While the power law itself seems confirmed, the initial assumptions made when deriving the power law, and indeed our fundamental understanding of turbulence, are being challenged. The classical view involves a gradual cascade of energy from the large towards decreasingly smaller scales, with isotropy existing at the small-scales.[13,14] However, studies indicate that these underlying assumptions in Kolmogorov's theory do not hold. That is, anisotropy of the small-scales is observed,[15,16] and direct scale interactions across the whole scale range exist with significant energy transfer to the small as well as the large scales.[17–19] A revised conceptual picture of the turbulent motions in physical space is thus needed, which, moreover, is consistent with the observed spectral scaling.

Here, we present a shear layer type flow structure that exhibits $-5/3$rd power scaling of its spectra in nearly all directions. This shear layer structure demonstrates how small-scale universality, small-scale anisotropy, and direct large-scale small-scale interaction can be consistent with the well-known spectral scaling.

Attempts at comprehending important aspects of turbulent flow have traditionally been made by introducing idealized flow models. Most of these models consist of a vortex of some sort,[20–22] which has been supported by observations of intense vorticity being predominantly concentrated in tubes.[23,24] While insightful in many ways, these single vortex models alone do not explain the $k^{-5/3}$ scaling of the energy spectrum E. For example, the Burgers vortex tube model gives $E \sim k^{-1}$,[25] while the Burgers vortex layer yields $E \sim k^{-2}$.[26] Rather, refinements of such models have required

a)Email: g.e.elsinga@tudelft.nl

introducing a random distribution of vortices of different sizes or shapes. Lundgren[25] was able to achieve a $k^{-5/3}$ spectrum using a spiral vortex model, but to do so he assumed a continuous distribution of self-similar structures at different stages of development (i.e., different sizes).[25,27] The concept of such an extended range of vortical structure sizes, however, conflicts with visualizations of vorticity structures in high Reynolds number turbulence, which display vortices nominally of similar size and non-uniformly distributed in space.[12] Moreover, the large-scale intense vorticity in numerical simulations appears to be blob-like and not self-similar to the tube-like small-scale vortices.[28] Furthermore, Yeung, Brasseur, and Wang[17] found evidence of a strong and direct coupling between the large and the small scales of motion in both physical and Fourier space, which is not accounted for in the mentioned conceptual models. Therefore, describing turbulence by individual vortices seems overly simplified and inaccurate. Rather, their spatial organization also needs to be taken into account.

Pirozzoli[29] considered the radial distribution of mean tangential velocity across vortex tubes in homogeneous isotropic turbulence. The resulting tangential velocity profiles deviated from the Burgers vortex tube model outside the vortex core, which again suggests the larger flow scales surrounding a vortex are important. Furthermore, the profiles showed an $r^{-2/3}$ decay with radial distance r. Assuming the velocity profiles are the same in all directions relative to the vortex, i.e., isotropy of the small-scales, the $k^{-5/3}$ scaling of the transverse spectrum was derived from the one-dimensional velocity profile. However, the assumption of small-scale isotropy is questionable,[15,16] as already pointed out.

More recent work has highlighted the importance of shear layer structures in turbulence.[30,31] In particular, such layers were argued to be dominant and universal features of small-scale turbulence based on instantaneous flow visualizations and the average flow associated with the local strain field.[31] The strain field governs turbulence production via vorticity stretching, hence defining a natural basis for studying turbulence. This strain field analysis revealed a shear layer coincident with stretched vortices (as shown in Fig. 1), which was found universally across a variety of turbulent flows including homogeneous isotropic turbulence and wall-bounded turbulence.[31] Moreover, this shear layer structure was shown in Ref. 31 to preserve the main characteristics related to the velocity gradient tensor in fully turbulent flows, notably the vorticity-intermediate strain alignment[32] and the teardrop shape of the joint-pdf of the velocity gradient tensor invariants.[33] In addition, the shear layer structure is consistent with, and details, the observed non-uniform spatial distribution of vortices in turbulent flow[12,34] and the anisotropy of the small-scales. Based on an evaluation of wall-bounded turbulence,

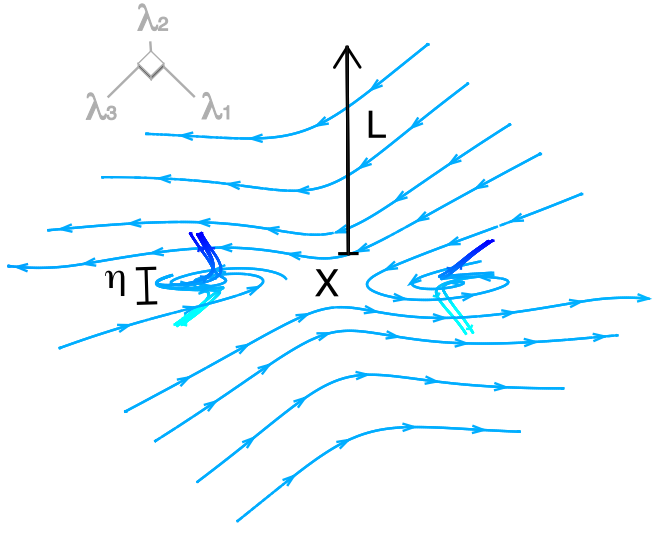

FIG. 1. The average flow associated with the local principal strain field around the point marked by X. Three-dimensional streamlines (blue) highlight a shear layer containing swirling motions that are being stretched in the direction of intermediate principal strain λ_2. The shear layer plane is at 45° with the most stretching straining direction λ_1 and the most compressive straining direction λ_3 and includes the λ_2 direction. The size of the core of the layer scales on the Kolmogorov length η, while the outer region scales on the macro-length L.[35]

the velocity field associated with this structure was, furthermore, shown to contain large and small turbulent length scales simultaneously,[35] as summarized in Fig. 1.

Given its universal appearance and consistency with relevant small-scale phenomenology, the shear layer structure obtained from the strain field analysis is a suitable model to represent turbulent motions in a simplified way. Taking it as a representative flow structure, we wonder how it contributes to the spectrum and whether the $k^{-5/3}$ energy spectrum scaling is satisfied.

Therefore, we examine the spectral content of the mentioned shear layer structure, which was derived from Direct Numerical Simulation (DNS) of homogeneous isotropic turbulence at two different Reynolds numbers. The first DNS dataset is at $Re_\lambda = 170$ (courtesy of A. A. Wray, CTR 2002), where Re_λ is the Reynolds number based on the Taylor micro-scale. It was computed using the same numerical scheme as in Ref. 24. The second dataset at $Re_\lambda = 433$ is from the Johns Hopkins University turbulence database.[36] Then, for each Reynolds number, the layer structure was obtained following the procedure introduced in Ref. 31. In this procedure, the fluctuating velocity field around a point is interpolated onto a new grid aligned with the local principal straining directions in that point, referred to as the strain eigenframe. These principal strain directions are given by the eigenvectors of the strain rate tensor, which is the symmetric part of the velocity gradient tensor. When defining the strain eigenframe, the intermediate principal straining direction is taken such that its inner product with the local vorticity vector is positive. These velocity fields on the strain eigenframe around individual points are finally averaged considering all points within the flow. The result (Fig. 1) represents the average three-dimensional flow velocity field around a point as seen when the observer is aligned with the local strain field. We emphasize the structure is not weak, even if it is an average. The peak velocity within the layer corresponds to 37%-58% of the root-mean-square velocity in the underlying turbulent flow, consistent with data in Ref. 35. This peak velocity is attained at around 10 Kolmogorov length scales from the center of the layer. As such, the present shear layer is an example of an intermittent, and highly dissipative small-scale structure, which features in the universal scaling laws proposed by She and Leveque.[37] While intense dissipation was imagined to be filamentary in that paper, later work showed the corresponding structure is actually pancake or sheet-like and is located adjacent to the vortex filaments.[34,38,39] Such sheet-like dissipation with neighboring vortical motion is again consistent with the present layer (Fig. 1), as discussed also in Ref. 31. Moreover, the present shear layer structure is persistent, which can be seen from the non-dimensional time scale T derived from the vorticity equation,

$$T = \|\omega\|^2 \left\| \frac{D\omega}{Dt} \right\|^{-1} = \|\omega\|^2 \|A\omega + \nu\nabla^2\omega\|^{-1}. \tag{1}$$

Here, ω is the vorticity vector, A is the velocity gradient tensor, and ν is the kinematic viscosity. At the center of the layer, T is of order 100. The large value of T indicates an approximate balance between production and dissipation of vorticity, which causes the material derivative of vorticity to be small in comparison to the vorticity magnitude. Hence, the shear layer flow is not perfectly steady, but its dynamics are very slow. In other words, the structure is persistent.

To obtain the longitudinal spectrum associated with the shear layer structure, velocity profiles are taken along lines intersecting the layer at the point of averaging, i.e., the origin of the strain eigenframe (Fig. 2(a)). From these profiles, the energy spectrum is computed for the velocity component parallel to each line of intersection. Here, we simply consider the spectrum of the layer structure itself, which demonstrates how such a structure contributes to the spectrum of a turbulent flow. The approach is different to the spectral theory of Hunt *et al.*,[30] which involves other additional structures impacting on and departing from the shear layer. In an isotropic turbulent flow that consists of many layer structures, each layer structure can have any orientation relative to the fixed world coordinates and consequently the longitudinal energy spectrum is averaged over all possible directions of intersection. However, in anisotropic flow, the structure will have a preferential orientation and therefore a fixed observer will probe it mainly along selected directions. This effect is simulated by considering only the intersections within a particular range of directions when averaging the spectrum. The different directional ranges used are partially overlapping and indicated in Fig. 2(a) by the colors on a unit sphere centered on the origin of the strain eigenframe. We have chosen finite size ranges, as opposed to spectra along individual lines of intersection, mainly to allow for certain (yet limited) randomness in the orientation

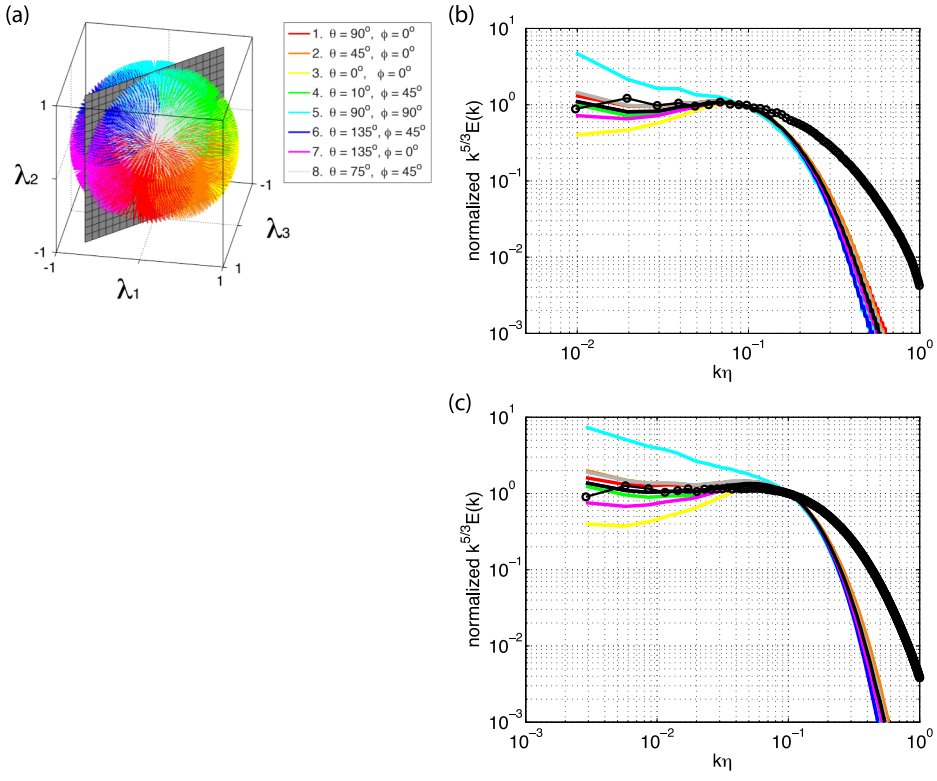

FIG. 2. Energy spectra taken along different directions through the average shear layer structure. (a) The spectrum is obtained along each colored line through the center of the layer, i.e., the origin of the strain eigenframe (λ_1, λ_2, λ_3). The colors indicate the different directional ranges over which the spectra are subsequently averaged. Each directional range describes a cone with a 40° half top angle. The cone axis' azimuthal, θ, and elevation angle, ϕ, with respect to the λ_1-λ_3 plane are listed in the legend. The orientation of the shear layer is shown by the grey plane for reference. (b) and (c) The resulting energy spectra $E(k)$, pre-multiplied by $k^{5/3}$, are plotted against wavenumber k normalized by the Kolmogorov length scale η. This way a plateau corresponds to a $k^{-5/3}$ scaling range in the energy spectra. (b) is for $Re_\lambda = 170$ while (c) represents $Re_\lambda = 433$. Furthermore, the pre-multiplied spectra are normalized to unity at $k\eta = 0.1$ to provide a straightforward comparison of the slopes. The color-coding corresponds to the directions in (a). The isotropic case, considering all directions in the averaging, is shown in black without symbols, while the actual turbulence spectrum is given in black with symbols. The $k^{-5/3}$ scaling range in the average shear layer and actual turbulence are found to overlap.

of the structure within the flow, and second to reduce numerical wiggles in the spectra associated with computing them from discretized velocity fields.

The resulting spectra at both Re_λ (Figs. 2(b)-2(c)) reveal a $k^{-5/3}$ scaling for the isotropic case as well as for most anisotropic cases, i.e., along most directions of intersection. Moreover, the wavenumber range for which this scaling holds is the same as for the actual turbulent flow. In anisotropic flows like boundary and mixing layers, an approximate statistical alignment of the shear layers with the mean flow is expected. It is, therefore, particularly significant that a $k^{-5/3}$ scaling is found along the shear layer structure (purple, color label 7). This demonstrates that such a turbulent structure can yield either a mean shear flow or an isotropic flow while maintaining a $k^{-5/3}$ spectrum at the same time. A single, arguably universal,[31] flow structure may thus explain both kinds of turbulent flow.

Notable exceptions to a $k^{-5/3}$ scaling are the spectra in the direction of intermediate principal strain and the most stretching strain. They, respectively, show a larger and a smaller relative contribution of the small wavenumbers. Furthermore, at high wavenumbers, beyond the $k^{-5/3}$ range, the spectra for the layer structure drop faster than the true turbulent spectrum, which is due to the averaging procedure used to obtain the layer structure. The corresponding difference in flow velocity at these scales remains small, as shown next.

In order to address the spectral differences at large wavenumbers, $k\eta > 10^{-1}$, we consider the longitudinal velocity profiles along the same lines of intersection used to determine the spectra.

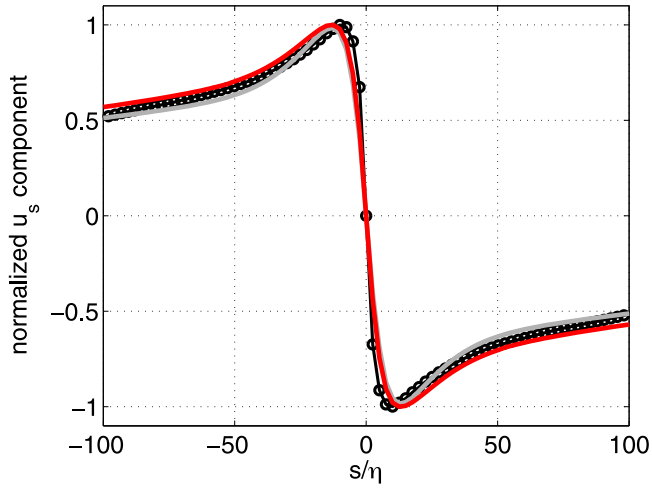

FIG. 3. Comparison of reconstructed longitudinal velocity profiles associated with the turbulence spectrum (black) and the shear layer spectrum averaged over all directions (gray). These velocity profiles were obtained from an inverse sine transform of the respective spectra. All sine waves were taken compressive and in-phase at the origin, which allows a further comparison with the actual velocity profile across the layer in the direction of the most compressive strain λ_3 (red). All profiles were normalized by their peak value.

The distance to the origin along such a line is denoted by s and the corresponding longitudinal component of velocity, i.e., the component in the direction of s, is given by u_s. The present average flow pattern associated with the local strain field has a 180° rotational symmetry due to the symmetry of the strain rate tensor on which it is based. Therefore, the longitudinal velocity profiles satisfy $u_s(s) = -u_s(-s)$ and can be represented by a discrete sine transform around the origin. Then to reconstruct the velocity profiles associated with the kinetic energy spectra, an inverse sine transform is performed using the spectral energy distributions at $Re_\lambda = 170$ presented in Fig. 2(b). All waves are assumed in-phase at the origin. Figure 3 compares the reconstructed longitudinal velocity profiles based on the actual turbulence spectrum (black line) and the shear layer spectrum averaged over all directions (gray line). The latter is taken as representative of the different shear layer spectra, which overlap with the turbulence spectrum in the $k^{-5/3}$ range while deviating at larger wavenumbers, $k\eta > 10^{-1}$ (Fig. 2(b)). Overall the comparison reveals very similar velocity profiles, though the location of the peak velocity is observed to shift slightly from $s/\eta = 10$ to 12. The shift clearly is smaller than the width of the present shear layer and the intense vortical structures in a turbulent flow, which are 6-10η in diameter.[24,40] The same analysis was repeated using the spectra at $Re_\lambda = 433$ (Fig. 2(c)), which yielded similar results. Therefore, we conclude that the observed spectral differences at large wavenumber have only a minor effect on the velocity profiles, and that the small-scales of motion inside the shear layer are well represented. Here, we define the small-scales *of motion* as the size of the smallest vortical motions within the turbulent flow (i.e., 6-10η[24,40]). Even smaller scales ($<6\eta$) still contribute to dissipation, but do not create an independent coherent motion. That means, the velocity gradients within the shear layer structure may be underestimated (due to averaging), but the flow structure/motion itself is well represented as shown in Figure 3.

When computing the reconstructed longitudinal velocity profiles from the spectra (Fig. 3), it was assumed that all sine waves are in-phase at the origin, i.e., the center of the shear layer. This assumption can be validated by comparing the reconstructed profiles with a velocity profile taken directly from the velocity field of the shear layer structure. Here, we consider the velocity profile along the direction of the most compressive strain, λ_3, which was shown to exhibit a $k^{-5/3}$ range in its associated spectrum (Fig. 2(b)). This velocity profile compares favorably with the profile reconstructed from the shear layer spectrum (Fig. 3, compare red and gray lines). Therefore, it is concluded that the assumption is appropriate and that the waves appear in phase at the origin. We interpret this as a further evidence for a direct interaction between the waves within the shear layer.

Approximating the shear layer as a jump in velocity, we can infer from Fourier analysis that the spatial waves, which decompose this jump, cover the full range of scales and will be in phase at the location of the jump. This implies that these waves interact in physical space at the location of the jumps or layers, which is in line with the above results. The direct scale interaction can also be explained in a different way. The nearly uniform velocity on each side of the shear layer, hence the velocity difference across the layer, is set by the large-scale motions outside the layer (Fig. 1). These outer motions correspond to the long tails in the velocity profiles ($s/\eta < -12$ and $s/\eta > 12$ in Fig. 3), whose length scales with the macroscopic length scale of the flow.[35] Therefore, a change in the velocity of the large-scale outer motions directly affects the velocity difference across the layer, which is, in fact, the velocity associated with the small-scales of motion contained inside the shear layer (Fig. 1). So there is a direct interaction between the scales.

In summary, the shear layer model contains all relevant turbulent length scales with relative amplitudes consistent with the well-known $k^{-5/3}$ energy spectrum scaling in actual turbulent flow. Moreover, the $k^{-5/3}$ spectrum scaling appeared when considering isotropic as well as anisotropic flow conditions, i.e., in isotropic and most of the anisotropic intersections of the layer. This is an important result, as the small-scales have been shown to remain anisotropic in high Reynolds number shear flow.[15] Furthermore, all spectral waves are in phase at the center of the shear layer, which we interpret as evidence for a direct interaction between the waves at that location. It presents a physical mechanism for the strong, direct coupling and energy transfer between scales observed in turbulent flow.[17] Additionally, the present shear layer structure was already shown to appear universally in different turbulent flows.[31] Hence, our results show how small-scale universality, small-scale anisotropy, and direct scale interaction can be reconciled with the $k^{-5/3}$ spectrum. The small scales of turbulent motion thus need not be isotropic and independent of the large scales to produce this spectral scaling, as is classically assumed.

[1] C. F. McKee and E. C. Ostriker, "Theory of star formation," Annu. Rev. Astron. Astrophys. **45**, 565–687 (2007).
[2] A. Chepurnov and A. Lazarian, "Extending the big power law in the sky with turbulence spectra from Wisconsin Hα Mapper data," Astrophys. J. **710**, 853–858 (2010).
[3] H. J. S. Fernando, "Fluid dynamics of urban atmospheres in complex terrain," Annu. Rev. Fluid Mech. **42**, 365–389 (2010).
[4] S. R. Hanna *et al.*, "Detailed simulations of atmospheric flow and dispersion in downtown Manhattan: An application of five computational fluid dynamics models," Bull. Am. Meteorol. Soc. **87**, 1713–1726 (2006).
[5] D. N. Ku, "Blood flow in arteries," Annu. Rev. Fluid Mech. **29**, 399–434 (1997).
[6] P. D. Stein and H. N. Sabbah, "Turbulent blood flow in the ascending aorta of humans with normal and diseased aortic valves," Circ. Res. **39**, 58–65 (1976).
[7] A. N. Kolmogorov, "The local structure of turbulence in incompressible viscous fluid for very large Reynolds number," Dokl. Akad. Nauk SSSR **30**, 301–305 (1941).
[8] A. N. Kolmogorov, "Dissipation of energy in the locally isotropic turbulence," Dokl. Akad. Nauk SSSR **32**, 16–18 (1941).
[9] A. M. Obukhov, "On the spectral energy distribution in a turbulent flow," Dokl. Akad. Nauk SSSR **32**, 22–24 (1941).
[10] H. L. Grant, R. W. Stewart, and A. Moillet, "Turbulence spectra from a tidal channel," J. Fluid Mech. **12**, 241–268 (1962).
[11] S. G. Saddoughi and S. V. Veeravalli, "Local isotropy in turbulent boundary layers at high Reynolds number," J. Fluid Mech. **268**, 333–372 (1994).
[12] T. Ishihara, T. Gotoh, and Y. Kaneda, "Study of high-Reynolds number isotropic turbulence by direct numerical simulation," Annu. Rev. Fluid Mech. **41**, 165–180 (2009).
[13] P. A. Davidson, *Turbulence: An Introduction for Scientists and Engineers* (Oxford University Press, 2004).
[14] S. B. Pope, *Turbulent Flows* (Cambridge University Press, 2000).
[15] X. Shen and Z. Warhaft, "The anisotropy of the small scale structure in high Reynolds number ($R_\lambda \sim 1000$) turbulent shear flow," Phys. Fluids **12**, 2976–2989 (2000).
[16] A. La Porta, G. A. Voth, A. M. Crawford, J. Alexander, and E. Bodenschatz, "Fluid particle accelerations in fully developed turbulence," Nature **409**, 1017–1019 (2001).
[17] P. K. Yeung, J. G. Brasseur, and Q. Wang, "Dynamics of direct large-small scale couplings in coherently forced turbulence: Concurrent physical- and Fourier-space views," J. Fluid Mech. **283**, 43–95 (1995).
[18] T. Aoyama, T. Ishihara, Y. Kaneda, M. Yokokawa, K. Itakura, and A. Uno, "Statistics of energy transfer in high-resolution direct numerical simulation of turbulence in a periodic box," J. Phys. Soc. Jpn. **74**, 3202–3212 (2005).
[19] L. Biferale, S. Musacchio, and F. Toschi, "Inverse energy cascade in three-dimensional isotropic turbulence," Phys. Rev. Lett. **108**, 164501 (2012).
[20] J. M. Burgers, "A mathematical model illustrating the theory of turbulence," Adv. Appl. Mech. **1**, 171–199 (1948).
[21] H. Tennekes, "Simple model for the small-scale structure of turbulence," Phys. Fluids **11**, 669–671 (1968).
[22] M. Rossi, F. Bottausci, A. Maurel, and P. Petitjeans, "A nonuniformly stretched vortex," Phys. Rev. Lett. **92**, 054504 (2004).
[23] Z.-S. She, E. Jackson, and S. A. Orszag, "Intermittent vortex structures in homogenous isotropic turbulence," Nature **344**, 226–228 (1990).
[24] J. Jimenez, A. A. Wray, P. G. Saffman, and R. S. Rogallo, "The structure of intense vorticity in isotropic turbulence," J. Fluid Mech. **255**, 65–90 (1993).

[25] T. S. Lundgren, "Strained spiral vortex model for turbulent fine structure," Phys. Fluids **25**, 2193–2203 (1982).
[26] D. I. Pullin and P. G. Saffman, "Vortex dynamics in turbulence," Annu. Rev. Fluid Mech. **30**, 31–51 (1998).
[27] K. Horiuti and T. Fujisawa, "The multi-mode stretched spiral vortex in homogenous isotropic turbulence," J. Fluid Mech. **595**, 341–366 (2008).
[28] T. Leung, N. Swaminathan, and P. A. Davidson, "Geometry and interaction of structures in homogeneous isotropic turbulence," J. Fluid Mech. **710**, 453–481 (2012).
[29] S. Pirozzoli, "On the velocity and dissipation signature of vortex tubes in isotropic turbulence," Physica D **241**, 202–207 (2012).
[30] J. C. R. Hunt, T. Ishihara, N. A. Worth, and Y. Kaneda, "Thin shear layer structures in high Reynolds number turbulence," Flow, Turbul. Combust. **92**, 607–649 (2014).
[31] G. E. Elsinga and I. Marusic, "Universal aspects of small-scale motions in turbulence," J. Fluid Mech. **662**, 514–539 (2010).
[32] W. T. Ashurst, A. R. Kerstein, R. M. Kerr, and C. H. Gibson, "Alignment of vorticity and scalar gradient with strain rate in simulated Navier-stokes turbulence," Phys. Fluids **30**, 2343–2353 (1987).
[33] A. Ooi, J. Martin, J. Soria, and M. S. Chong, "A study of the evolution and characteristics of the invariants of the velocity-gradient tensor in isotropic turbulence," J. Fluid Mech. **381**, 141–174 (1999).
[34] F. Moisy and J. Jimenez, "Geometry and clustering of intense structures in isotropic turbulence," J. Fluid Mech. **513**, 111–133 (2004).
[35] L. Wei, G. E. Elsinga, G. Brethouwer, P. Schlatter, and A. V. Johansson, "Universality and scaling phenomenology of small-scale turbulence in wall-bounded flows," Phys. Fluids **26**, 035107 (2014).
[36] Y. Li, E. Perlman, M. Wan, Y. Yang, C. Meneveau, R. Burns, S. Chen, A. Szalay, and G. Eyink, "A public turbulence database cluster and applications to study Lagrangian evolution of velocity increments in turbulence," J. Turbul. **9**, 1–29 (2008).
[37] Z.-S. She and E. Leveque, "Universal scaling laws in fully developed turbulence," Phys. Rev. Lett. **72**, 336–339 (1994).
[38] J. M. Chacin and B. J. Cantwell, "Dynamics of a low Reynolds number turbulent boundary layer," J. Fluid Mech. **404**, 87–115 (2000).
[39] B. Ganapathisubramani, K. Lakshminarasimhan, and N. T. Clemens, "Investigation of threedimensional structure of fine scales in a turbulent jet by using cinematographic stereoscopic particle image velocimetry," J. Fluid Mech. **598**, 141–175 (2008).
[40] Y. Kaneda and T. Ishihara, "High-resolution direct numerical simulation of turbulence," J. Turbul. **7**, 1–17 (2006).